HHS Public Access

Author manuscript

Pharm Res. Author manuscript; available in PMC 2021 December 10.

Published in final edited form as:

Pharm Res. 2016 April ; 33(4): 909–921. doi:10.1007/s11095-015-1837-5.

Absorption and Clearance of Pharmaceutical Aerosols in the Human Nose: Effects of Nasal Spray Suspension Particle Size and Properties

Alex Rygg[1], **Michael Hindle**[2], **P. Worth Longest**[1,2,*]

[1]Department of Mechanical and Nuclear Engineering, Virginia Commonwealth University, Richmond, VA

[2]Department of Pharmaceutics, Virginia Commonwealth University, Richmond, VA

Abstract

Purpose: The objective of this study was to use a recently developed nasal dissolution, absorption, and clearance (DAC) model to evaluate the extent to which suspended drug particle size influences nasal epithelial drug absorption for a spray product.

Methods: Computational fluid dynamic (CFD) simulations of mucociliary clearance and drug dissolution were used to calculate total and microscale epithelial absorption of drug delivered with a nasal spray pump. Ranges of suspended particle sizes, drug solubilities, and partition coefficients were evaluated.

Results: Considering mometasone furoate as an example, suspended drug particle sizes in the range of 1–5 μm did not affect the total nasal epithelial uptake. However, the microscale absorption of suspended drug particles with low solubilities was affected by particle size and this controlled the extent to which the drug penetrated into the distal nasal regions.

Conclusions: The nasal-DAC model was demonstrated to be a useful tool in determining the nasal exposure of spray formulations with different drug particle sizes and solubilities. Furthermore, the model illustrated a new strategy for topical nasal drug delivery in which drug particle size is selected to increase the region of epithelial surface exposure using mucociliary clearance while minimizing the drug dose exiting the nasopharynx.

Keywords

Nasal spray suspensions; drug particle dissolution; nasal clearance; nasal drug absorption; post-deposition particle tracking

INTRODUCTION

The establishment of bioequivalence between an innovator and generic pharmaceutical product is required by the US FDA for the generic product to enter the marketplace (1). The introduction of generic products is typically viewed as a favorable path to control the

[*]**Corresponding Author:** Dr. P. Worth Longest, Virginia Commonwealth University, 401 West Main Street, P.O. Box 843015, Richmond, VA 23284-3015, Phone: (804)-827-7023, Fax: (804)-827-7030, pwlongest@vcu.edu.

cost of medications, which have been steadily increasing in the US market (2). For nasal spray suspensions, a weight of evidence approach is taken for testing bioequivalence to ensure both the safety and efficacy of the products (1). However, evaluation and comparison of these drug products poses significant challenges to regulators due to the complex relationship between nasal deposition producing a local effect and the systemic drug concentrations that are conventionally used to compare the rate and extent of absorption (1, 3). The overall process for establishing bioequivalence of locally acting nasal suspensions requires a combination of data including equivalent *in vitro* performance, equivalent local delivery established by a clinical endpoint, equivalent systemic exposure, together with demonstration of device and formulation sameness (1). It is unclear if the current methods that are employed to characterize nasal spray suspension products for regulatory purposes are able to detect variability in local and systemic drug absorption with regards to the changes in the physicochemical properties of a formulation as well as regional nasal deposition patterns (4, 5). In addition, studies have not previously considered the size of the drug particles in a suspension formulation, which also may have a significant effect on these bioequivalence metrics. Particle size of suspended drug particles is expected to be coupled with drug-specific properties, such as solubility and partitioning behavior (6), in affecting both local and systemic exposure.

With regards to nasal suspension formulations, it could be expected that the dissolution of corticosteroid drug particles will be the rate limiting step in the overall absorption process (7). Dissolution testing of corticosteroids has shown that drug particle size, solubility, and formulation have significant effects on their dissolution kinetics (6, 7). For these molecules, decreasing the drug particle size or increasing drug solubility in mucus results in faster dissolution rates (7). Additionally, small changes in formulation composition can lead to significantly altered *in vitro* dissolution rates (6). While these previous *in vitro* studies have quantified dissolution rates for commonly used corticosteroid formulations suitable for pulmonary or nasal administration in a physiological volume of fluid, they did not take into account the clearance and absorption that would occur in the human airways.

Total nasal and systemic drug exposure for nasal sprays is dependent, among other factors, on regional nasal deposition patterns. Nasal deposition patterns from spray pumps have been reported using both computational fluid dynamics (CFD) (8–13) and *in vitro* experiments (14–18). These studies show generally low deposition efficiencies in the posterior nasal cavity, where absorption occurs. Considering nasal and respiratory epithelial cellular absorption in general, several groups have modeled vapor uptake in the respiratory airways (19–22), showing varied absorption rates that depend on the vapor partition coefficients. Additionally, CFD and pharmacokinetic data of gas absorption have been linked in animal models (23), providing an additional correlation in determining local and systemic exposure. However, CFD simulations have not yet examined the effect of drug particle size and solubility on overall drug absorption after deposition in the nasal airway surface liquid (ASL) lining. A coupled model of nasal clearance and drug dissolution would thus be useful in understanding the effects of suspension properties on total and regional nasal epithelial uptake.

We previously developed a new CFD model that simulates the coupled effects of particle dissolution, drug absorption and nasal clearance for corticosteroid nasal spray suspension products (24). This nasal-DAC (dissolution, absorption, and clearance) model utilizes an anatomically-accurate surface model of the nasal cavity, and was shown to simulate particle clearance that reflected *in vivo* rates for healthy adults. The overall ASL clearance rate was shown to have a significant impact on drug absorption over long time scales (up to 1 hour). Additionally, a large amount of variability in drug absorption was observed when considering that particles deposited in the nasal vestibule could either be carried to the back of the nose over long time scales, or be removed by sneezing or nose blowing. Overall, the nasal-DAC model has significant potential for evaluating the factors that affect nasal drug absorption for both locally acting and systemically targeted nasal drug products, and can reduce the reliance on *in vivo* testing during formulation development.

The objective of this study is to use the nasal-DAC model to evaluate the parameter space in which suspended drug particle size has an effect on total and regional nasal drug absorption following administration of a suspension nasal spray product. This is accomplished by considering a range of suspended drug particle sizes from 1–5 μm, as well as varying the drug solubility and partition coefficient at the nasal epithelium. Nasal sprays consist of coarse liquid droplets (20–100 μm) emitted from a spray pump or other device. The spray droplets act as a vehicle to transport the active drug molecule as suspended un-dissolved drug particles. In this study, the nasal-DAC model is further developed and used to analyze the effect of suspended drug particle size on nasal epithelial drug absorption. If suspended drug particle size is shown to have an effect on absorption, then methods of characterizing the drug particle size *in situ* in formulated nasal sprays may be an important new consideration for establishing bioequivalence using *in vitro* methods, even when the spray plume characteristics and droplet sizes are equivalent. In contrast, if the suspended drug particle size is shown to be unimportant, this finding could potentially reduce the requirements and costs associated with developing generic nasal spray drug products. Most likely, this answer is a complex function of the molecular properties of the drug in terms of solubility and partition coefficient taken together with the intended purpose of the nasal spray product (local or systemic action), which motivates the use of the complex and newly introduced (24) nasal-DAC model.

MATERIALS AND METHODS

Overview

The overall methodology, shown in Figure 1, starts with CFD simulations of nasal spray deposition in a three-dimensional model of the human nasal cavity, with regional deposition predictions validated in the previous study of Rygg and Longest (24). The spray droplet deposition locations in the 3D nasal cavity (Figure 1a) were then translated onto an anatomically-accurate surface model of the nose (Figure 1b) for use in CFD simulations of drug particle dissolution and drug absorption (Figure 1c). The concept behind this methodology is that the initial spray deposition patterns will affect the dissolution and absorption rates of the suspended drug particles, and that the post-deposition physics are best addressed by a separate clearance model capable of resolving the spatial and

temporal drug concentration profiles. Using a velocity field (24) that realistically models nasal clearance rates *in vivo* for healthy adults (18), simulations of drug particle transport, dissolution, and diffusion were carried out, allowing for calculations of microscale drug absorption at the epithelium. In this study a corticosteroid, mometasone furoate (MF), was used as a representative drug with a range of suspended particle sizes evaluated. In addition, the effect of varying the drug solubility and partition coefficient were considered and evaluated to determine their effects on microscale and cumulative uptake, as described in the following sections.

Surface Model and CFD Velocity Field

The anatomy of the nasal surface model along with the validated (24) CFD-predicted ASL velocity field are shown in Figure 2. To create the surface model, morphometric data of the nasal cavity from Xi et al. (13, 25) was mapped to a flat surface whose transverse length corresponded to the combined cross-sectional perimeter of the left and right nasal airways at a given distance from the nostril. Also taken into account in the model are the physiological differences in the regions corresponding to the nasal vestibule (NV), middle passages (MP), and the nasopharynx (NP). This model (Figure 2) therefore represents an anatomically representative version of the nasal cavity that extends from the nostrils to the throat. The computed ASL velocity field (24) takes into account the unciliated region in the NV (26), where the ASL velocity is close to zero. In the ciliated posterior middle passage region of the nose (MP), an average ASL mucociliary clearance rate of 5–6 mm/min can be seen, which is representative of average *in vivo* conditions (27–29).

As described by Rygg and Longest (24), the ASL velocity field in the CFD model represented the physical mucociliary clearance mechanisms acting in both mucus (gel) and periciliary (sol) layers. The nasal cilia beat within the sol layer, and on the forward strokes the tips of the cilia contact and propel the gel layer (30, 31). Because the cilia are attached at the epithelial surface and have a highest velocity at the mucus interface, the periciliary velocity profile was assumed to resemble that shown in Figure 1c. Furthermore, as the viscosity of the gel layer is very high relative to the periciliary layer, we assumed the velocity in the mucus layer to be constant in the wall-normal direction, which is also shown in Figure 1c. A flow field that satisfies these requirements was created by injecting epithelial liquid into the domain to maintain the desired cross-sectional velocity profile. In the ciliated region of the nose (i.e., MP), the magnitude of the mass source was specified such that, after solving the Navier-Stokes transport equations, the average velocity in the MP was close to the 5–6 mm/min range reported in the literature (5, 27–29). The ASL layer was assumed to be present in the NV, but fluid injection was not present. Importantly, the nature of the fluid injection in the MP region led to a natural velocity transition region between the NV and MP. A resulting slow transport of NV ASL into the MP occurred and is in agreement with previous reports of nasal clearance “phases”, where the quick removal of posteriorly-deposited drug is succeeded by the slow clearance of particles deposited in the non-ciliated nasal vestibule (32, 33).

The ASL velocity field was previously verified as reasonable by Rygg and Longest (24) through comparisons with *in vivo* radiolabel clearance data from Shah et al. (18). In the

study by Shah et al. (18), a nasal spray device was used to deposit radiolabel tracer into the noses of human subjects, and scintigraphic measurements determined the rate of ASL clearance by mucociliary transport. For the verification study, CFD simulations utilized the velocity field described above and an initial “radiolabel” deposition profile matching that reported by Shah et al. (18). Transient calculations of radiolabel transport and clearance over a simulation time of 6 hours allowed for direct comparison with experimental time points. Results showed that the drug remaining in the CFD nasal model during the simulated time closely matched the corresponding values reported by Shah et al. (18), with <10% relative difference between the two clearance profiles at all data points (24). Thus, the velocity field in the CFD model is expected to reasonably represent drug particle clearance from the nasal cavity and include effects of local velocity and expected acceleration of the ASL in the posterior portions of the MP.

Particle Dissolution, Absorption, and Clearance Model

In the current computational model, the drug particles dissolve according to the Noyes-Whitney equation as they move through the nasal cavity, expressed as

$$\frac{dm}{dt} = \frac{A D_{mucus}(C_s - C_b)}{h} \quad (1)$$

where A is the surface area of the particle, D_{mucus} is the diffusion coefficient of the drug in mucus (or ASL), C_s is the solubility of the drug, C_b is the concentration in the bulk phase, and h is the diffusion layer thickness. Since the effective radius of a mometasone molecule is very small (~1 nm), the diffusion coefficient of the dissolved drug in mucus is approximately equal to its diffusion coefficient in water (34). The aqueous diffusion coefficient of MF was calculated by the Hayduk and Laudie equation (35) to be D_{mucus} = 4.3e-6 cm^2/s; all other drug properties (e.g. solubility, density, etc.) were taken from the Nasonex® product information (36). For a particle radius < 30 μm, the diffusion layer thickness h can be approximated as the particle radius that changes with time as the drug dissolves (37). Two solubilities (C_s) were considered; a value of C_s = 0.02 mg/mL is representative of MF, while a higher value of C_s = 0.2 mg/mL is characteristic of a more soluble inhaled corticosteroid such as flunisolide (7). The bulk phase concentration (C_b) field was actively updated in the simulations to represent the evolving environment around each particle including particle-to-particle interactions.

The code governing the dissolution behavior of the solid drug particles in the nasal-DAC model was previously validated (24) with dissolution data provided by Arora et al. (7) for three corticosteroids with widely varying solubilities. Arora et al. (7) measured particle dissolution rates in a Transwell® system, which contained a donor dissolution compartment bounded by a permeable membrane and basal receptor compartment. To validate the CFD particle dissolution code, a computational domain corresponding to the Transwell® system was created, and CFD simulations of particle dissolution were carried out for three different drugs (24). Over a simulation time of 1.5 hours, the CFD predictions of dissolved drug mass were compared to the measurements by Arora et al. (7), and good agreement was found for each of the corticosteroids (24). As the solubility of the different drugs increased, so did the dissolution rate, leading to a greater amount of drug permeating the membrane at

each time point. Thus, the user-defined-functions implemented in the current simulations are expected to accurately predict concentration-limited particle dissolution behavior for each of the solubilities considered.

In the nasal-DAC model, the behavior of the dissolved drug was governed by the advection-diffusion equation, i.e.,

$$\frac{\partial}{\partial t}(\rho Y_i) + \nabla \cdot \left(\rho \vec{v} Y_i\right) = \nabla \cdot \left(\rho D_{i,m} \nabla Y_i\right) + S_i \tag{2}$$

where ρ is the fluid density, Y_i is the mass fraction of species i, $\vec{v}$ is the fluid velocity, $D_{i,m}$ is the mass diffusion coefficient of the drug, and the source term S_i accounts for the microscale addition of drug into the bulk phase from the dissolving particles. The advection-diffusion equation was solved in the mucus and periciliary layers (ASL) shown in Figure 1 with boundary conditions described below.

When calculating drug uptake at the epithelium, differences in nasal cell types were taken into account. The anterior third of the nose (i.e., NV) is characterized by keratinized, stratified squamous epithelium (5, 30, 38) and is therefore unlikely to absorb any significant amount of drug. A zero-gradient boundary condition for the drug was therefore applied to the epithelium in this region. In the posterior region of the nose, which is covered with respiratory and olfactory epithelium, a mixed boundary condition was applied that accounted for drug partitioning between the aqueous ASL layer and the epithelial cell membranes. This type of mixed boundary condition, which has been utilized in previous studies (20, 21, 39, 40), was derived by combining conservation of mass at the ASL/epithelium interface and the definition of the equilibrium partition coefficient. Specifically, conservation of mass at the interface is given by

$$D_{muc}\frac{\partial C_{muc}}{\partial x_n}\bigg|_i = D_{mem}\frac{\partial C_{mem}}{\partial x_n}\bigg|_i \tag{3}$$

where D_{muc} and D_{mem} are the drug diffusion coefficients in the ASL and cell membrane, respectively; C_{muc} and C_{mem} are the drug concentrations in the ASL and cell membrane at the interface *i*, respectively; and x_n is the direction normal to the epithelial surface. Because the cell membrane represents a lipid phase, and the ASL represents an aqueous phase, the octanol/water equilibrium partition coefficient was approximated by

$$K_{o/w} = \frac{C_{mem}}{C_{muc}}\bigg|_i \tag{4}$$

where $K_{o/w}$ is the octanol/water drug partition coefficient.

Assuming a linear concentration profile in the cell membrane and zero concentration within the cell, a combination of Equations (3) and (4) yields an ASL-phase mixed boundary condition at the epithelial surface, given by

$$\left.\frac{\partial C_{muc}}{\partial x_n}\right|_i - \left.\frac{D_{mem}K_{o/w}}{D_{muc}t_{mem}}C_{muc}\right|_i = 0 \quad (5)$$

where t_{mem} is the thickness of the epithelial cell membrane, and the other variables are defined as before. Due to the complex nature of the cell membrane, it is likely that the drug concentration profile is not perfectly linear across the membrane. However, given the extremely small length scale associated with the membrane, this approximation was deemed appropriate for this stage of model development. It can be noted from Equation (5) that increasing the octanol/water partition coefficient leads to a zero concentration boundary condition at the epithelium, while a vanishingly small partition coefficient can be represented by a zero-gradient boundary condition. Two different values of $K_{o/w}$ were considered in this study. A partition coefficient of 5000 is appropriate for MF (41), which has a very high relative affinity for the lipid phase. Drugs with higher water-solubility tend to have lower partition coefficients, and a value of $K_{o/w} = 2$ is used to represent flunisolide (42).

The current CFD-based DAC model provides the new capability to predict microscale, regional and total nasal deposition and subsequent epithelial absorption, with several current assumptions. The term microscale refers to the dissolution and epithelial absorption of individual particles and particle groups occurring on the finest resolved scale of the model. In the current simulations, the microscale dimension is ~80 μm, compared with a respiratory epithelial cell with a characteristic dimension of ~10 μm. Regional deposition refers to broad sections of the nasal airways, such as the nasal vestibule (NV), middle passages (MP), and the nasopharynx (NP). Because a flattened surface model (Figure 1b) of the nasal cavity is used in the DAC simulations, some regions of the nasal cavity such as the middle meatus or olfactory region are not currently identified. Instead, the DAC model provides microscale dose estimates at different penetration depths into the nasal cavity (Figure 2), which can be mapped to the general NV, MP, and NP regions.

Drug Particle Injection

Drug particles were injected into the surface model domain according to previous 3D CFD calculations of droplet deposition from a nasal spray device. These CFD simulations were validated with the *in vitro* experiments of Azimi et al. (43), which implemented a Nasonex® (Merck & Co., Summit, NJ) spray pump, containing MF as the suspended drug product, and an *in vitro* rapid prototype airway geometry identical to that used in the computational simulations. Results of the CFD simulations and *in vitro* experiments showed deposition fractions of approximately 90% in the NV and 10% in the MP using the defined conditions. To translate the droplet deposition locations from the 3D geometry to the surface model, the axial distance of each droplet from the nostril was calculated. This distance was translated to a location relative to the nostril on the surface model, where a suspended particle starting point was specified. Additionally, the spray droplet size was taken into account by weighting the number of drug particles at each location in the surface model by the droplet mass, such that the mass deposition fractions in the 3D and surface models were in agreement. Using these initial starting points, simulations of particle mucociliary clearance, dissolution, and drug absorption were carried out for a deposited drug dose of 50 μg of MF.

Numerical Methods

Computational fluid dynamics simulations were run using ANSYS Fluent 15 (ANSYS Inc., Canonsburg, PA) coupled with user-defined functions for particle dissolution and epithelial cell absorption. A steady-state flow solution was obtained using the SIMPLEC algorithm for pressure-velocity coupling, and all transport equations were discretized to 2nd order accuracy in space. A converged solution was obtained when all mass and momentum residuals dropped by at least three orders of magnitude and did not change with further iterations. The mesh resolution was found to be sufficient, as demonstrated by a grid refinement study. Figure 3 shows cumulative epithelial drug absorption from particles deposited in the MP using two meshes of different resolutions. Refining the mesh by a factor of 1.5 spanning the ASL layer resulted in a negligible change (0.68% difference) in cumulative uptake after 10 minutes (Figure 3). This indicates that the current mesh resolution accurately captures the dissolution and drug transport physics of rapidly-dissolving particles. Using the calculated ASL flow field shown in Figure 2, transient simulations of particle transport, dissolution, and species diffusion were carried out for a total simulation time of one hour at a time step of 1 s, requiring n = 3600 time step advancements with approximately 5 solution iterations at each time step.

RESULTS

Drug Particle Trajectories

Trajectories of individual drug particles are displayed in Figure 4 and colored according to the current drug particle diameter as dissolution in the ASL is occurring over a time period of 60 minutes. Length of the pathlines indicates distance traveled by the drug particles over the simulated time period. These drug particles were initially delivered as a coarse droplet aerosol released from a Nasonex® (Merck & Co., Summit, NJ) spray pump. As described in the Methods, deposition locations of the droplets, also simulated with CFD, defined the starting locations of the suspended drug particles in the ASL. The suspended drug particles in Figure 4 had an initial monodisperse diameter of 3 μm and were released at a random, uniformly distributed depth in the mucus. It is unknown how deeply the aerosol drug particles penetrate the nasal mucus layer upon deposition, but it is likely a complex factor of particle surface properties (44, 45). The effect of this penetration distance on overall epithelial uptake was investigated in the previous study by Rygg and Longest (46). It was found that if the surface properties of the particles inhibited them from burrowing into the mucus layer (i.e. they remained on the ASL surface), the drug was carried to the back of the nose more quickly by the higher velocity in this region (see Figure 1). This resulted in a moderate increase in drug absorption over 1 hour. Although the particle penetration distances are formulation-dependent, the randomly distributed depths used in the current study were chosen because this methodology provided a drug clearance rate that best agreed with the measured *in vivo* data (18).

As shown in Figure 4, drug particles in the faster velocity region (towards the central posterior region of the nose) get carried further before fully dissolving, while those drug particles deposited in the stagnant regions remain where they are deposited. At the end of one hour, all particles in the MP were fully dissolved, but some undissolved particles

remained in the NV. As discussed in the next section, particles near the interface between the NV and MP were transported a very short distance before dissolving due to the low ASL velocities in this transition region. It is expected that the limited motion of these particles will result in a disproportionate epithelial uptake of the medication in the MP near the NV with little drug progressing to the posterior nasal cavity and nasopharynx.

Effect of Particle Size

An important goal of the current simulations was to examine the effect of drug particle size on cumulative total nasal uptake and regional absorption. Figure 5 represents cumulative drug uptake by the nasal epithelium as a function of time for different suspended drug particle sizes. The data is plotted as a percentage of the total deposited dose (50 μg). It should be noted that, even after an hour, undissolved drug particles were still present in the nasal vestibule due to solubility-limited dissolution and slow clearance from this region. Additionally, for all particle sizes considered, a negligible amount of drug exited at the back of the throat; for the largest particle size (5 μm), only 0.08% of the deposited drug would be swallowed by the patient, and this amount decreases for smaller particle sizes. The results show that smaller particles are able to dissolve more quickly than larger ones, resulting in a faster initial uptake of drug over the first ~5–10 minutes (Figure 5). This quick initial uptake corresponds to drug particles that are deposited in the posterior region of the nose, where the respiratory epithelium is located. Additionally, since more of the small drug particles dissolve prior to reaching the nasopharynx and exiting the flow domain, a slightly larger cumulative uptake after an hour can be seen as drug particle size decreases. The 1 μm drug particles had 50.8% cumulative uptake at one hour versus 48.1% for the 5 μm particles, which may be difficult to distinguish using a clinical endpoint due to *in vivo* variability. The slower, steady uptake for all sizes after ≈10 minutes arises from drug deposited in the NV, which is carried to the respiratory epithelium by the motion of the posterior ASL. Because drug particle size has no effect on solubility, the amount of dissolved drug in the NV is independent of initial particle diameter. As a result, the rate of drug advection from the front of the nose is constant for all particle sizes. Thus, a small drug particle size results in a quick initial uptake of drug, but at longer time scales the cumulative uptake is relatively insensitive to particle size. These findings would indicate that total epithelial uptake is not dependent on drug particle size in the diameter range of 1 – 5 μm. However, it is expected that drug particle size will influence the location of uptake within the nose as larger drug particles are transported further before complete dissolution and absorption occurs.

Despite the small differences in cumulative total nasal drug uptake for different particle sizes at times longer than 10 minutes, microscale uptake patterns changed significantly as the particle size was varied. To illustrate this, an absorption enhancement factor (AEF) was defined for the microscale drug uptake at the epithelium. Similar to the deposition enhancement factor proposed by Longest et al. (47) and Balásházy et al. (48), this AEF describes the ratio of the drug uptake per unit area in a computational cell to the drug uptake per unit area over the entire epithelium. Mathematically, the AEF is defined by

$$AEF = \frac{m_{cell}/A_{cell}}{m_{total}/A_{epithelium}} \quad (6)$$

where m_{cell} is the cumulative drug uptake in a computational cell, A_{cell} is the face area of the computational cell at the epithelium, m_{total} is the total cumulative drug uptake, and $A_{epithelium}$ is the surface area of the entire epithelium. An AEF of 100 indicates that the microscale epithelial surface dose per unit area ($\mu g/cm^2$) is 100-fold higher than the total nasal epithelial surface dose considered over the entire surface area of the nose. Similarly, an AEF of 10^{-2} indicates that 100-fold less surface dose per unit area is deposited in a region compared with the value that would be predicted if the deposited dose was averaged over the entire epithelial surface. The AEF can also be used to predict the microscale surface dose per unit area based on the product of the AEF value and total dose per unit surface area.

Contour plots of the AEF for different particle sizes show that a much larger portion of the epithelium is exposed to drug when the initial particle size is increased (Figure 6). Small particles dissolve relatively quickly, and most of the drug is absorbed at the initial particle deposition locations. Because large particles dissolve more slowly, they are carried further by ciliary motion, exposing a greater amount of epithelial surface area to the drug. The maximum recorded AEF value was 425 for the case of 1 μm particles and was reduced to a maximum value of 166 for the case of 5 μm particles.

For the delivery of nasal corticosteroids and other topical medications, both the improved surface coverage and the reduced hot spot formation provided by the larger 5 μm particles appears to be advantageous. An optimal particle size therefore exists that is large enough to allow clearance to better spread the medication and small enough to allow for near full nasal absorption of the medication.

Effect of Drug Solubility

Drug solubility was shown to have a modest effect on cumulative total nasal uptake rates at the epithelium (Figure 7). When the aqueous solubility of the drug was increased from 0.02 mg/mL to 0.2 mg/mL, the particles dissolved much more quickly, as indicated by the fast uptake rate within the first minute (Figure 7). This was expected given the influence of C_s in Equation (1). However, even at this higher solubility, the cumulative total uptake was relatively independent of initial particle size; and the slow, steady uptake rate at longer time scales indicates solubility-limited dissolution in the NV. Once again, at the higher solubility, the amount of drug exiting the back of the throat was negligible, as the particles had sufficient time to dissolve before reaching the nasopharynx.

Importantly, the AEF parameter showed less dependence on the initial particle size when the solubility was increased (Figure 8). In contrast to Figure 6, the AEF contours at the higher solubility remained very similar among the different particle sizes due to the fast dissolution and rapid drug uptake rates. Because the drug particles dissolved much more quickly in these simulations, the ASL velocity was insufficient to carry even the large particles to the NP, leading to decreased drug absorption in this region.

Effect of Drug Partition Coefficient at the Epithelium

When the octanol/water partition coefficient ($K_{o/w}$) of the drug was changed from 5000 to 2, a slight decrease in cumulative total nasal uptake was seen for all particle sizes, because the drug was not absorbed as readily at the epithelium (Figure 9). Noticeably, the uptake rates within the first 10 minutes are much slower when this lower partition coefficient is considered. Still, for $K_{o/w} = 2$, the initial particle size had only a small effect on cumulative total nasal uptake. For illustrative purposes, results are also shown for a value of $K_{o/w} = 5\times10^{-3}$, which would represent a very hydrophilic drug. For this very small partition coefficient, the cumulative total nasal uptake was greatly reduced compared to the lipophilic corticosteroids. At $K_{o/w} = 2$, the amount of drug exiting the back of the throat was again very small, despite the decreased absorption at the epithelium (only 0.2% was swallowed for the largest drug particle size). However, for the case of $K_{o/w} = 5\times10^{-3}$ and an initial particle size of 3 μm, 27.6% of the deposited drug was swallowed due to the significantly reduced epithelial uptake.

At the lower value of $K_{o/w} = 2$, contours of the AEF showed a strong dependency on particle size, where larger particles distributed drug over a greater portion of the epithelium (Figure 10). Additionally, by comparing Figure 6 to Figure 10, it can be seen that decreasing the partition coefficient results in drug absorption over more surface area for a given initial particle size. Correspondingly, the AEF contour for $K_{o/w} = 5\times10^{-3}$ shows an almost uniform distribution of drug, where the maximum AEF value is only ≈2.5.

DISCUSSION

The results of this study quantify, for the first time, how suspended drug particle size, solubility, and partitioning behavior in a suspension nasal spray formulation are significant factors for achieving a desired therapeutic effect. After a simulation time of 1 hour, the cumulative epithelial uptake was relatively independent of particle size. Interestingly, this behavior has also been observed using bronchial epithelia for steroid particle sizes ranging from 0.4 to 3.3 μm (49). However, AEF microscale contours indicate that small drug particles dissolve quickly and deliver drug to the site of deposition, whereas larger particles are carried along further by the cilia and are absorbed over a greater surface area. Therefore, small particles appear to work well if the goal is quick absorption into the systemic circulation. In contrast, larger particles may be required for treating localized conditions or targeting hard to reach nasal regions such as the back portions of the MP and NP.

Increasing the aqueous solubility of a formulation results in very quick dissolution and uptake of the drug particles that are deposited in the posterior regions of the nose. However, contours of the AEF show that a relatively small portion of the epithelium is exposed to drug at this increased solubility, even for large suspended drug particles. As a result, formulations that are highly soluble in ASL may not be preferable for targeting hard to reach more distal areas, as the suspended particles may dissolve before the cilia have an opportunity to transport them to the site of action.

Decreasing the octanol/water partition coefficient of the drug results in a slightly lower total dose absorbed at the epithelium, although further pharmacokinetic studies are needed

to determine the corresponding effect on the plasma concentration profile. Regional uptake patterns showed that, for a given initial particle size, drug was absorbed over a greater surface area as the partition coefficient was decreased. This relationship between partitioning behavior and chemical absorption has been previously reported in the context of odorant deposition and patterning (40). The study by Lawson et al. (40) showed that chemicals that are not readily absorbed by the mucosal layer are distributed almost uniformly in the nasal cavity. In contrast, significant chromatographic-like separation was observed for odorants that were readily absorbed. Relating this to the current results, decreasing the octanol/water partition coefficient of a drug can lead to more uniform absorption and increased uptake in the posterior regions of the nose. However, significantly reducing the value of $K_{o/w}$ can lead to a large amount of drug being swallowed by the patient.

Figures 11 and 12 provide a visual illustration of these results with regard to their influence on microscale absorption effects. These contour plots are shaded according to the percent of the epithelial surface area where AEF < 0.1 or AEF > 5. An AEF value outside the range of 0.1<AEF<5 indicates that drug uptake in a computational cell is significantly less than or greater than the overall uptake per unit area. In other words, extreme AEF values in Figures 6, 8, and 10 represent “hot” and “cold” spots, or non-uniform absorption patterns. Therefore, the contour plots in Figures 11 and 12 give a visual representation of the extent to which drug is distributed evenly (or unevenly) over the epithelium as a function of initial particle size, drug solubility, and partition coefficient including the effects of clearance, dissolution, and absorption. Red regions indicate that an increasing amount of drug was absorbed over relatively small, isolated regions, and that microscale deposition patterns and absorption effects are important. Blue regions, on the other hand, show that drug was distributed over a wider surface area, and that significant absorption can be expected even in regions where the drug was not initially deposited as a result of ASL motion. Figure 11 indicates that suspension formulations with large drug particle sizes or low aqueous solubility perform better when a greater portion of the epithelial tissue requires treatment. Likewise, Figure 12 shows that a large particle size or small partition coefficient leads to greater distribution of drug over the epithelial surface. However, cumulative total nasal uptake must still be taken into account together with the total systemic dose, which is important in bioequivalence assessments.

One area of active research involves the development of mucus penetrating nanoparticles for nasal drug delivery (50–52). These particles, which are designed to avoid adhesion to mucins and quickly traverse the mucus layer, have shown promise for quickly delivering drugs that may otherwise be cleared by mucociliary action. However, the results of this study show that these quickly-absorbed particles may not be optimal for treating certain conditions such as sinusitis, which would rely on mucociliary clearance to carry the drug particles to a targeted region. In this light, new technologies (such as nanoparticles) would greatly improve drug delivery when quick systemic uptake is desired, but may have some previously unexplored disadvantages when the target application is treating the nasal tissue as with conventional nasal spray products.

Respirable microspheres are also at the forefront of aerosol drug delivery technology (53, 54), and can be used to sustain drug release, prolong retention in the airways, or enhance

drug absorption. Given the results of the current simulations, where certain nasal spray formulations may not meet the therapeutic needs of the patient due to particle size or solubility, these types of microspheres could be used to modify the properties of current suspensions to more effectively deliver the active ingredient. Outcomes of this approach may result in enhanced targeting of the sinuses, more consistent drug delivery between individuals, or faster uptake of drugs that act systemically.

The current results promote a new approach for delivering topical locally acting nasal products and provide insight into the effects of formulation variables on both total nasal and systemic exposure. The intent of this new delivery approach is to use a combination of dissolution, clearance and absorption to maximize the surface area covered by the drug product. In this approach, suspended drug particle size should be selected for a specific therapeutic molecule (with a known solubility and partition coefficient) as large enough to allow for mucociliary clearance to deliver the medication throughout the MP and NP and small enough to minimize wastage through exiting the NP and swallowing. Based on results of this study, a 5 μm MF particle diameter appears advantageous to maximize drug absorption throughout the nose and may improve outcomes compared with a smaller particle size of approximately 1 μm. The maps provided as Figures 11 and 12 can be used to specify optimal particle sizes for other medications based on knowledge of the drug solubility and partitioning behavior. Of course, this newly proposed approach of improving nasal drug delivery requires that the clearance system be functioning, which is not always the case in respiratory diseases and conditions (55–59). Changes to mucus layer thickness and clearance velocity can be integrated into the model to assess the resulting effects on epithelial absorption.

Taking advantage of clearance to improve nasal drug delivery is in partial contrast with the current approach of bioadhesive formulations (4, 60, 61). These formulations typically implement excipients that increase the mucus viscosity and/or bind mucus to the epithelial surface to increase the time available for dissolution and absorption of the drug. This bioadhesive approach is beneficial in many applications where low solubilities and low uptake are significant issues (53, 54). However, the current study points out that binding the particles to the site of deposition does not allow for spreading the medication to the posterior nasal regions via clearance. Rygg and Longest (24) indicate that diffusional transport of nasal spray suspension and dissolved drug was negligible. Current nasal spray devices deposit a majority of the medication to the anterior portion of the nose. As a result, bio-adhesion approaches may not provide sufficient doses of nasal targeted medications to the distal nasal regions. It therefore becomes important to combine current bioadhesive approaches with more advanced aerosol delivery targeting that can deposit the drug initially throughout the nose. In contrast with bio-adhesion, properly selected initial particle sizes combined with methods to enhance and control dissolution and uptake may improve topical drug delivery to the entire nasal cavity, even when the initial deposition profile is poorly distributed within the nose.

Streamlining the regulatory approach to nasal spray bioequivalence testing would be advantageous, and the computational methodology presented here may be useful in reducing the burden of *in vitro*, pharmacokinetic and clinical studies, due to its ability to simulate

local and systemic drug uptake for a variety of suspension nasal spray formulation properties. By utilizing data provided by *in vitro* and *in vivo* methods (6, 7, 14, 18, 62–64), this *in silico* approach can provide an efficient, and perhaps improved technique to evaluate nasal spray products which can be used alone or in combination with other conventional bioequivalence methods.

Although the current CFD model provides a better understanding of the relationship between nasal spray suspension properties and drug absorption, several limitations should be noted. First, the current model represents a simplified surface of the complex three dimensional nasal airways, and is therefore unable to isolate specific regions of the nasal cavity. That is, at this stage, the simplified surface model is unable to show if drug enters the sinuses or is deposited on the olfactory epithelium (which is a region of interest for drugs that act on the central nervous system and are transported across the blood brain barrier (65, 66)). Furthermore, the current model neglects the potential spreading of the nasal spray droplets after deposition (67–69). This spreading could have the ability to alter the initial distribution of suspended drug particles and the AEF contours seen in Figure 6. These physics could be included in future versions of the model to more accurately predict the fate of the droplets and subsequent epithelial drug absorption. It is also noted that, because the ASL is comprised mostly of water, the solubility values (C_s) are based on aqueous drug solubilities. However, the actual solubility of a drug in a complex *in vivo* ASL environment may differ from that in an aqueous buffered solution. Future developments of the model would ideally use precise drug solubilities in mucus, providing more accurate results. In addition to simplifying the properties of the drug, this study also considered a monodisperse suspension particle size for each simulation; however, commercial suspension formulations contain polydisperse drug particles suspended within the spray droplets. Finally, the model in its current form calculates the drug mass that is absorbed at the epithelium, but does not calculate the plasma concentration – time profiles. This makes it difficult to fully assess the effect of the drug partition coefficient on overall systemic dosage. A pharmacokinetics (PK) model is planned as an additional component to the current system, and would simulate the amount of drug that enters both the epithelial cells and the systemic circulation, allowing a one-to-one comparison of nasal deposition profiles and blood concentration of a nasal spray product for the first time.

As topics of future work, the current model will be extended to include more anatomical features (e.g. the sinuses) for simulating targeted nasal drug delivery. The model will also include a pharmacokinetic component, which will allow for the assessment of drug bioavailability and the full effects of partitioning behavior. This PK model will use *in vivo* data of inhaled MF bioavailability (70, 71) for development and validation, creating an efficient computational method for determining post-deposition plasma concentrations.

CONCLUSION

Results from the nasal-DAC model showed that differences in nasal spray suspension properties, including suspended drug particle size, can lead to varying regional uptake patterns. Using results such as these, nasal spray formulations can be optimized to treat specific conditions. For instance, small suspended particles work well if the goal is rapid

dissolution and absorption into the systemic circulation. Otherwise, for local treatment of nasal tissue or targeting drug delivery to the back of the nose, properly-sized larger particles perform better because they are carried further by the cilia and spread medication over a wider surface area due to clearance. Similarly, drugs with high aqueous solubility dissolve very quickly, and may not be optimal for treating nasal conditions. Considering MF as a specific example, results of the current study show that suspended drug particle size in the range of 1–5 μm is not important in terms of total nasal epithelial cell uptake. However, the primary particle size becomes very important if uptake in different regions of the nasal cavity is to be considered in assessing bioequivalence of these locally acting drugs as a surrogate for clinical endpoint studies. Improved coverage of the nasal epithelial surface was observed with a 5 μm drug particle size compared with 1 μm, with a negligible change in total drug absorption. Finally, for the delivery of locally acting topical medications like MF, the current study illustrates for the first time the use of properly sized suspended particles together with clearance to spread the medication over a majority of the nasal MP and NP regions. Based on these results, the newly developed nasal-DAC model can be used to efficiently investigate the relationship between nasal spray properties and drug absorption, allowing for improved treatment and formulation development.

ACKNOWLEDGMENTS

Dr. Geng Tian is gratefully acknowledged for his part in developing the NMT and nasal spray pump model during his time as a postdoc at Virginia Commonwealth University and Mandana Azimi for her critical review of the manuscript. This study was supported by Award U01 FD004570 and Contract HHSF223201310223C from the US FDA. The content is solely the responsibility of the authors and does not necessarily represent the official views of the US FDA.

ABBREVIATIONS

AEF	absorption enhancement factor
ASL	airway surface liquid
CFD	computational fluid dynamics
DAC	dissolution-absorption-clearance
MF	mometasone furoate
PK	pharmacokinetic

References

1. Li BV, Jin F, Lee SL, Bai T, Chowdhury B, Caramenico HT, et al. Bioequivalence for Locally Acting Nasal Spray and Nasal Aerosol Products: Standard Development and Generic Approval. The AAPS Journal. 2013;15(3):875–83. [PubMed: 23686396]
2. Davit BM, Nwakama PE, Buehler GJ, Conner DP, Haidar SH, Patel DT, et al. Comparing Generic and Innovator Drugs: A Review of 12 Years of Bioequivalence Data from the United States Food and Drug Administration. Annals of Pharmacotherapy. 2009;43(10):1583–97.
3. Suman JD, Laube BL, Dalby R. Validity of in vitro Tests on Aqueous Spray Pumps as Surrogates for Nasal Deposition, Absorption, and Biologic Response. Journal of Aerosol Medicine. 2006;19(4):510–21. [PubMed: 17196079]

4. Turker S, Onur E, Ozer Y. Nasal Route and Drug Delivery Systems. Pharmacy World and Science. 2004;26(3):137–42. [PubMed: 15230360]
5. Pires Ai, Fortuna A, Alves G, Fal1 ao Ai. Intranasal Drug Delivery: How, Why and What For? Journal of Pharmacy and Pharmaceutical Sciences. 2009;12(3):288–311. [PubMed: 20067706]
6. Buttini F, Miozzi M, Balducci AG, Royall PG, Brambilla G, Colombo P, et al. Differences in Physical Chemistry and Dissolution Rate of Solid Particle Aerosols from Solution Pressurised Inhalers. International Journal of Pharmaceutics. 2014;465(1):42–51. [PubMed: 24491530]
7. Arora D, Shah KA, Halquist MS, Sakagami M. In vitro Aqueous Fluid-Capacity-Limited Dissolution Testing of Respirable Aerosol Drug Particles Generated from Inhaler Products. Pharmaceutical Research. 2010;27(5):786–95. [PubMed: 20229134]
8. Schroeter JD, Kimbell JS, Asgharian B. Analysis of Particle Deposition in the Turbinate and Olfactory Regions Using a Human Nasal Computational Fluid Dynamics Model. Journal of Aerosol Medicine. 2006;19(3):301–13. [PubMed: 17034306]
9. Shi H, Kleinstreuer C, Zhang Z. Modeling of Inertial Particle Transport and Deposition in Human Nasal Cavities with Wall Roughness. Journal of Aerosol Science. 2007;38(4):398–419.
10. Liu Y, Matida EA, Johnson MR. Experimental Measurements and Computational Modeling of Aerosol Deposition in the Carleton-Civic Standardized Human Nasal Cavity. Journal of Aerosol Science. 2010;41(6):569–86.
11. Inthavong K, Ge Q, Se CMK, Yang W, Tu JY. Simulation of Sprayed Particle Deposition in a Human Nasal Cavity Including a Nasal Spray Device. Journal of Aerosol Science. 2011;42(2):100–13.
12. Schroeter JD, Garcia GJM, Kimbell JS. Effects of Surface Smoothness on Inertial Particle Deposition in Human Nasal Models. Journal of Aerosol Science. 2011;42(1):52–63. [PubMed: 21339833]
13. Xi J, Si X, Kim JW, Berlinski A. Simulation of Airflow and Aerosol Deposition in the Nasal Cavity of a 5-Year-Old Child. Journal of Aerosol Science. 2011;42(3):156–73.
14. Kelly JT, Asgharian B, Kimbell JS, Wong Ba. Particle Deposition in Human Nasal Airway Replicas Manufactured by Different Methods. Part I: Inertial Regime Particles. Aerosol Science and Technology. 2004;38(11):1063–71.
15. Kelly JT, Asgharian B, Kimbell JS, Wong Ba. Particle Deposition in Human Nasal Airway Replicas Manufactured by Different Methods. Part II: Ultrafine Particles. Aerosol Science and Technology. 2004;38(11):1072–9.
16. Garcia GJM, Tewksbury EW, Wong Ba, Kimbell JS. Interindividual Variability in Nasal Filtration as a Function of Nasal Cavity Geometry. Journal of Aerosol Medicine and Pulmonary Drug Delivery. 2009;22(2):139–55. [PubMed: 19422314]
17. Shah SA, Dickens CJ, Ward DJ, Banaszek AA, George C, Horodnik W. Design of Experiments to Optimize an In Vitro Cast to Predict Human Nasal Drug Deposition. Journal of Aerosol Medicine and Pulmonary Drug Delivery. 2014;26(0):1–9.
18. Shah SA, Berger RL, McDermott J, Gupta P, Monteith D, Connor A, et al. Regional Deposition of Mometasone Furoate Nasal Spray Suspension in Humans. Allergy and Asthma Proceedings. 2015;36(1):48–57. [PubMed: 25562556]
19. Kimbell JS, Subramaniam RP. Use of Computational Fluid Dynamics Models for Dosimetry of Inhaled Gases in the Nasal Passages. Inhalation Toxicology. 2001;13(5):325–34. [PubMed: 11295865]
20. Zhang Z, Kleinstreuer C, Kim CS. Transport and Uptake of MTBE and Ethanol Vapors in a Human Upper Airway Model. Inhalation Toxicology. 2006;18(3):169–84. [PubMed: 16399659]
21. Tian G, Longest PW. Development of a CFD Boundary Condition to Model Transient Vapor Absorption in the Respiratory Airways. Journal of Biomechanical Engineering. 2010;132(5):051003. [PubMed: 20459204]
22. Tian G, Longest PW. Transient Absorption of Inhaled Vapors into a Multilayer Mucus-Tissue-Blood System. Annals of Biomedical Engineering. 2010;38(2):517–36. [PubMed: 19826954]
23. Bush ML, Frederick CB, Kimbell JS, Ultman JS. A CFD PBPK Hybrid Model for Simulating Gas and Vapor Uptake in the Rat Nose. Toxicology and Applied Pharmacology. 1998;150(1):133–45. [PubMed: 9630462]

24. Rygg A, Longest PW. Absorption and Clearance of Pharmaceutical Aerosols in the Human Nose: Development of a CFD Model. Journal of Aerosol Medicine and Pulmonary Drug Delivery. 2015; In press.
25. Xi J, Longest PW. Numerical Predictions of Submicrometer Aerosol Deposition in the Nasal Cavity Using a Novel Drift Flux Approach. International Journal of Heat and Mass Transfer. 2008;51(23–24):5562–77.
26. Fry FA, Black A. Regional Deposition and Clearance of Particles in the Human Nose. Journal of Aerosol Science. 1973;4(2):113–24.
27. Illum L Nasal Drug Delivery - Possibilities, Problems and Solutions. Journal of Controlled Release. 2003;87(1–3):187–98. [PubMed: 12618035]
28. Mistry A, Stolnik S, Illum L. Nanoparticles for Direct Nose-to-Brain Delivery of Drugs. International Journal of Pharmaceutics. 2009;379(1–2):146–57. [PubMed: 19555750]
29. Ugwoke MI, Agu RU, Verbeke N, Kinget R. Nasal Mucoadhesive Drug Delivery: Background, Applications, Trends and Future Perspectives. Advanced Drug Delivery Reviews. 2005;57(11):1640–65. [PubMed: 16182408]
30. Beule AG. Physiology and Pathophysiology of the Paranasal Sinuses. GMS Current Topics in Otorhinolaryngology - Head and Neck Surgery. 2010;9.
31. Quraishi MS, Jones NS, Mason J. The Rheology of Nasal Mucus: A Review. Clinical Otolaryngology & Allied Sciences. 1998;23(5):403–13. [PubMed: 9800075]
32. McLean J, Bacon J, Mathews K, Thrall J, Banas J, Hedden J, et al. Distribution and Clearance of Radioactive Aerosol on the Nasal Mucosa. Rhinology. 1984;22(1):65–75. [PubMed: 6328631]
33. Djupesland PG. Nasal Drug Delivery Devices: Characteristics and Performance in a Clinical Perspective - A Review. Drug Delivery and Translational Research. 2013;3(1):42–62. [PubMed: 23316447]
34. Cu Y, Saltzman WM. Mathematical Modeling of Molecular Diffusion Through Mucus. Advanced Drug Delivery Reviews. 2009;61(2):101–14. [PubMed: 19135488]
35. Gulliver JS. Introduction to Chemical Transport in the Environment: Cambridge University Press; 2007.
36. Merck & Co. Nasonex Product Monograph. http://www.merck.ca/assets/en/pdf/products/NASONEX-PM_E.pdf.
37. Sugano K, Okazaki A, Sugimoto S, Tavornvipas S, Omura A, Mano T. Solubility and Dissolution Profile Assessment in Drug Discovery. Drug Metabolism and Pharmacokinetics. 2007;22(4):225–54. [PubMed: 17827779]
38. Schipper NGM, Verhoef JC, Merkus FWHM. The Nasal Mucociliary Clearance: Relevance to Nasal Drug Delivery. Pharmaceutical Research. 1991;8(7):807–14. [PubMed: 1924131]
39. Keyhani K, Scherer PW, Mozell MM. A Numerical Model of Nasal Odorant Transport for the Analysis of Human Olfaction. Journal of Theoretical Biology. 1997;186(3):279–301. [PubMed: 9219668]
40. Lawson M, Craven B, Paterson E, Settles G. A Computational Study of Odorant Transport and Deposition in the Canine Nasal Cavity: Implications for Olfaction. Chemical Senses. 2012;37(6):553–66. [PubMed: 22473924]
41. U.S. Food and Drug Administration. Nasonex Product Information. http://www.accessdata.fda.gov/drugsatfda_docs/label/2002/20762s11lbl.pdf.
42. U.S. Pharmacopeia. Flunisolide Safety Data Sheet. http://www.usp.org/pdf/EN/referenceStandards/msds/1274505.pdf.
43. Azimi M, Longest PW, Hindle M. Towards Clinically Relevant In Vitro Testing of Locally Acting Nasal Spray Suspension Products. Respiratory Drug Delivery Europe. 2015.
44. Gehr P, Schürch S, Berthiaume Y, HOF VI, Geiser M. Particle Retention in Airways by Surfactant. Journal of Aerosol Medicine. 1990;3(1):27–43.
45. Gehr P, Green F, Geiser M, Hof VI, Lee M, Schürch S. Airway Surfactant, A Primary Defense Barrier: Mechanical and Immunological Aspects. Journal of Aerosol Medicine. 1996;9(2):163–81. [PubMed: 10163349]

46. Rygg A, Longest PW. Absorption and Clearance of Pharmaceutical Aerosols in the Human Nose: Development of a CFD Model. Journal of Aerosol Medicine and Pulmonary Drug Delivery. In review.
47. Longest PW, Vinchurkar S, Martonen T. Transport and Deposition of Respiratory Aerosols in Models of Childhood Asthma. Journal of Aerosol Science. 2006;37(10):1234–57.
48. Balashazy I, Hofmann W, Heistracher T. Computation of Local Enhancement Factors for the Quantification of Particle Deposition Patterns in Airway Bifurcations. Journal of Aerosol Science. 1999;30(2):185–203.
49. Haghi M, Traini D, Young P. In vitro Cell Integrated Impactor Deposition Methodology for the Study of Aerodynamically Relevant Size Fractions from Commercial Pressurised Metered Dose Inhalers. Pharmaceutical Research. 2014;31(7):1779–87. [PubMed: 24549816]
50. Lai SK, Wang YY, Hanes J. Mucus-Penetrating Nanoparticles for Drug and Gene Delivery to Mucosal Tissues. Advanced Drug Delivery Reviews. 2009;61(2):158–71. [PubMed: 19133304]
51. Lai SK, Suk JS, Pace A, Wang YY, Yang M, Mert O, et al. Drug Carrier Nanoparticles that Penetrate Human Chronic Rhinosinusitis Mucus. Biomaterials. 2011;32(26):6285–90. [PubMed: 21665271]
52. Ensign LM, Schneider C, Suk JS, Cone R, Hanes J. Mucus Penetrating Nanoparticles: Biophysical Tool and Method of Drug and Gene Delivery. Advanced Materials. 2012;24(28):3887–94. [PubMed: 22988559]
53. Sakagami M, Byron PR. Respirable Microspheres for Inhalation. Clinical Pharmacokinetics. 2005;44(3):263–77. [PubMed: 15762769]
54. Pereswetoff-Morath L Microspheres as Nasal Drug Delivery Systems. Advanced Drug Delivery Reviews. 1998;29(1–2):185–94. [PubMed: 10837588]
55. Illum L Nasal Clearance in Health and Disease. Journal of Aerosol Medicine. 2006;19(1):92–9. [PubMed: 16551220]
56. Bond S, Hardy J, Wilson C, . Deposition and Clearance of Nasal Sprays. The 2nd International Congress of Biopharmaceutics and Pharmacokinetics; 1984; Salamanca.
57. Rosen EJ, Calhoun KH. Alterations of Nasal Mucociliary Clearance in Association with HIV Infection and the Effect of Guaifenesin Therapy. The Laryngoscope. 2005;115(1):27–30. [PubMed: 15630360]
58. Surico G, Muggeo P, Mappa L, Muggeo V, Conti V, Lucarelli A, et al. Impairment of Nasal Mucociliary Clearance After Radiotherapy for Childhood Head Cancer. Head & Neck. 2001;23(6):461–6. [PubMed: 11360307]
59. Ho JC, Chan KN, Hu WH, Lam WK, Zheng L, Tipoe GL, et al. The Effect of Aging on Nasal Mucociliary Clearance, Beat Frequency, and Ultrastructure of Respiratory Cilia. American Journal of Respiratory and Critical Care Medicine. 2001;163(4):983–8. [PubMed: 11282777]
60. Illum L Nasal Drug Delivery: New Developments and Strategies. Drug Discovery Today. 2002;7(23):1184–9. [PubMed: 12547019]
61. Patton JS, Brain JD, Davies La, Fiegel J, Gumbleton M, Kim K-J, et al. The Particle has Landed - Characterizing the Fate of Inhaled Pharmaceuticals. Journal of Aerosol Medicine and Pulmonary Drug Delivery. 2010;23, Supple:S71–S87. [PubMed: 21133802]
62. Al-Ghananeem AM, Sandefer EP, Doll WJ, Page RC, Chang Y, Digenis GA. Gamma Scintigraphy for Testing Bioequivalence: A Case Study on Two Cromolyn Sodium Nasal Spray Preparations. International Journal of Pharmaceutics. 2008;357(1):70–6. [PubMed: 18329197]
63. Bur M, Huwer H, Muys L, Lehr C-M. Drug Transport Across Pulmonary Epithelial Cell Monolayers: Effects of Particle Size, Apical Liquid Volume, and Deposition Technique. Journal of Aerosol Medicine and Pulmonary Drug Delivery. 2010;23(3):119–27. [PubMed: 20073555]
64. Henning A, Schneider M, Nafee N, Muijs L, Rytting E, Wang X, et al. Influence of Particle Size and Material Properties on Mucociliary Clearance from the Airways. Journal of Aerosol Medicine and Pulmonary Drug Delivery. 2010;23(4):233–41. [PubMed: 20500091]
65. Illum L Transport of Drugs from the Nasal Cavity to the Central Nervous System. European Journal of Pharmaceutical Sciences. 2000;11(1):1–18. [PubMed: 10913748]

66. Hanson LR, Frey WH. Intranasal Delivery Bypasses the Blood-Brain Barrier to Target Therapeutic Agents to the Central Nervous System and Treat Neurodegenerative Disease. BMC Neuroscience. 2008;9 Suppl 3:S5.

67. Shanahan M The Spreading Dynamics of a Liquid Drop on a Viscoelastic Solid. Journal of Physics D: Applied Physics. 1988;21(6):981.

68. Jacqmin D Contact-Line Dynamics of a Diffuse Fluid Interface. Journal of Fluid Mechanics. 2000;402:57–88.

69. Dussan E On the Spreading of Liquids on Solid Surfaces: Static and Dynamic Contact Lines. Annual Review of Fluid Mechanics. 1979;11(1):371–400.

70. Affrime MB, Cuss F, Padhi D, Wirth M, Pai S, Clement RP, et al. Bioavailability and Metabolism of Mometasone Furoate following Administration by Metered-Dose and Dry-Powder Inhalers in Healthy Human Volunteers. The Journal of Clinical Pharmacology. 2000;40(11):1227–36. [PubMed: 11075308]

71. Daley-Yates P, Kunka R, Yin Y, Andrews S, Callejas S, Ng C. Bioavailability of Fluticasone Propionate and Mometasone Furoate Aqueous Nasal Sprays. European Journal of Clinical Pharmacology. 2004;60(4):265–8. [PubMed: 15114430]

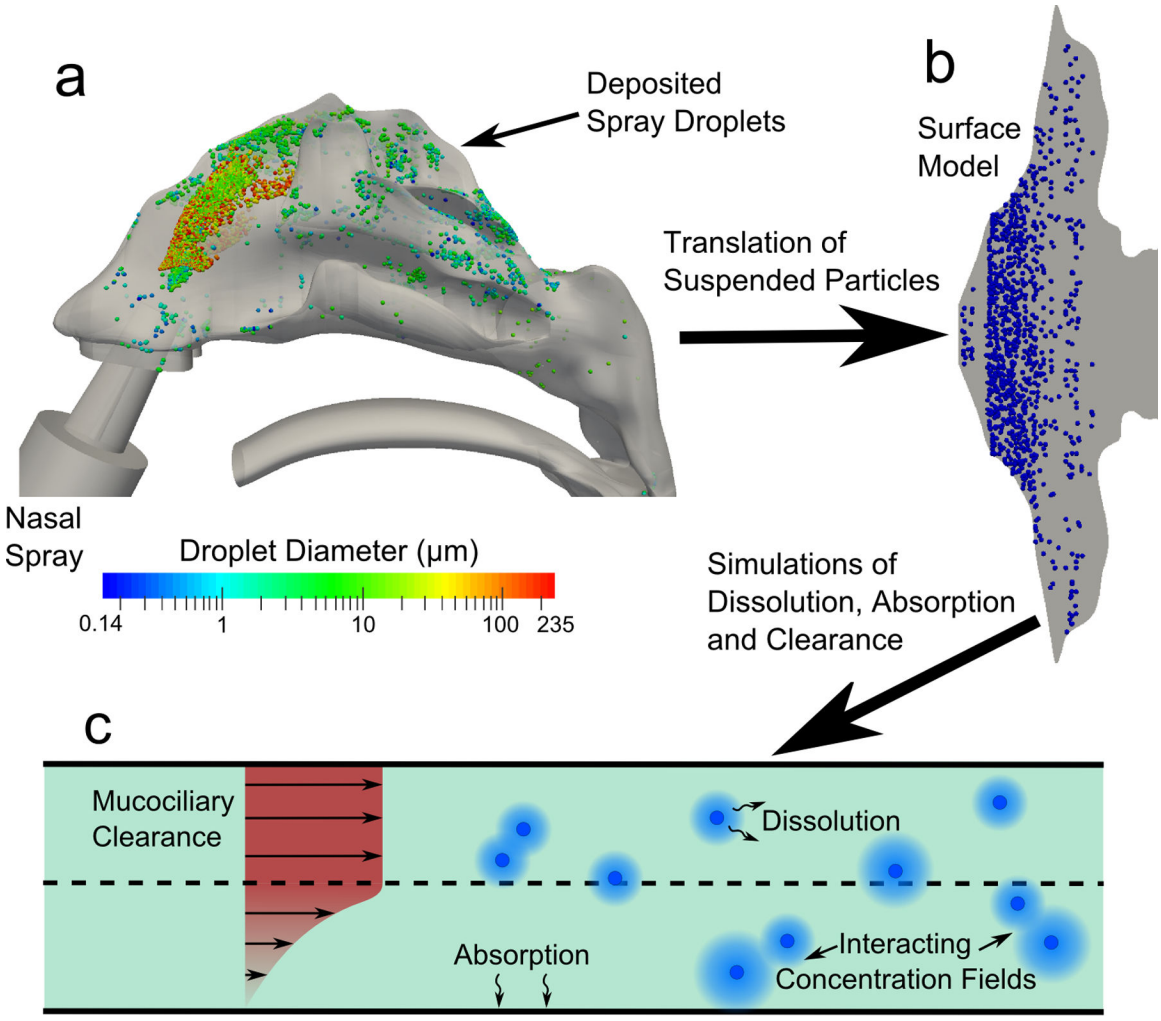

Figure 1.

The overall methodology for conducting the CFD simulations is shown. Particle deposition data in the (a) 3D model of the nose from a commercial nasal spray was mapped onto the (b) surface-based model. CFD simulations were conducted using this model and accounted for (c) particle advection due to mucociliary clearance, particle dissolution and diffusion, and drug absorption at the epithelial surface.

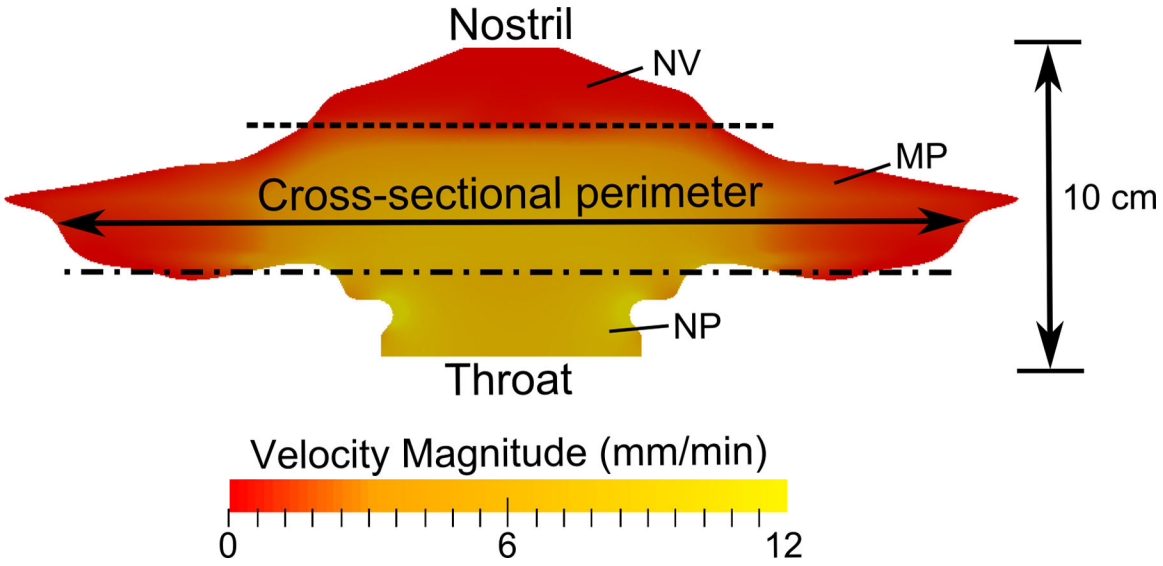

Figure 2.

The surface model of the nasal cavity is shown, where the lateral length corresponds to the cross-sectional perimeter of the airway. The dotted lines indicate the separation between the nasal vestibule (NV), middle passages (MP), and nasopharynx (NP) regions.

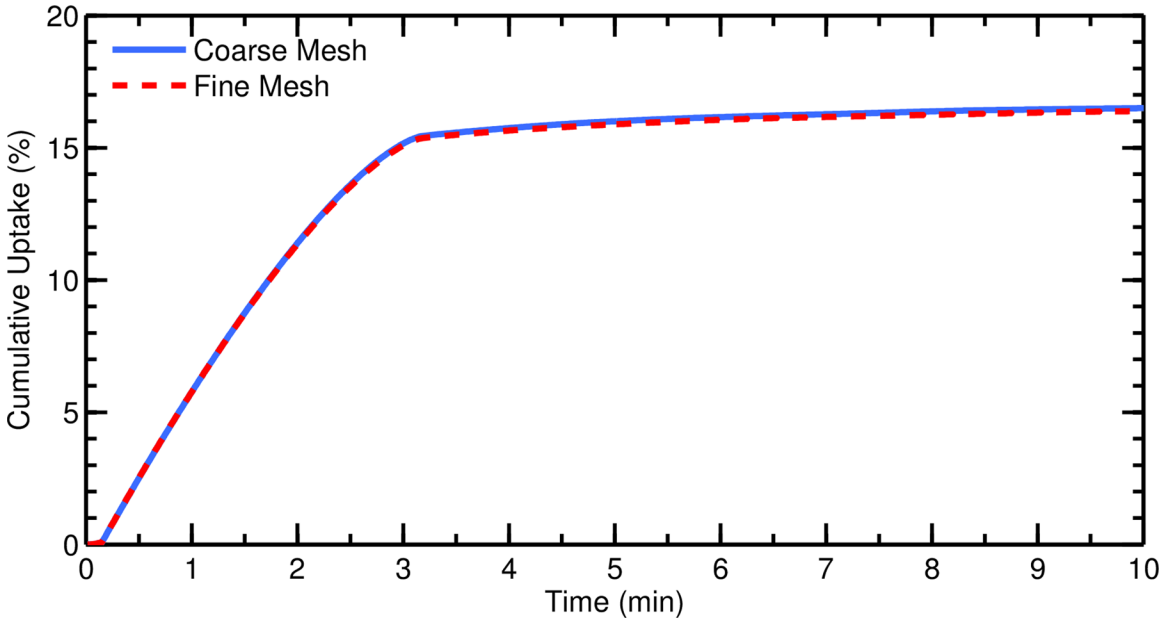

Figure 3.

Cumulative total nasal drug uptake at the epithelium over time is shown for two meshes of different resolutions (with a refinement ratio of 1.5 spanning the ASL layer). Results are shown as a percentage of total injected drug mass.

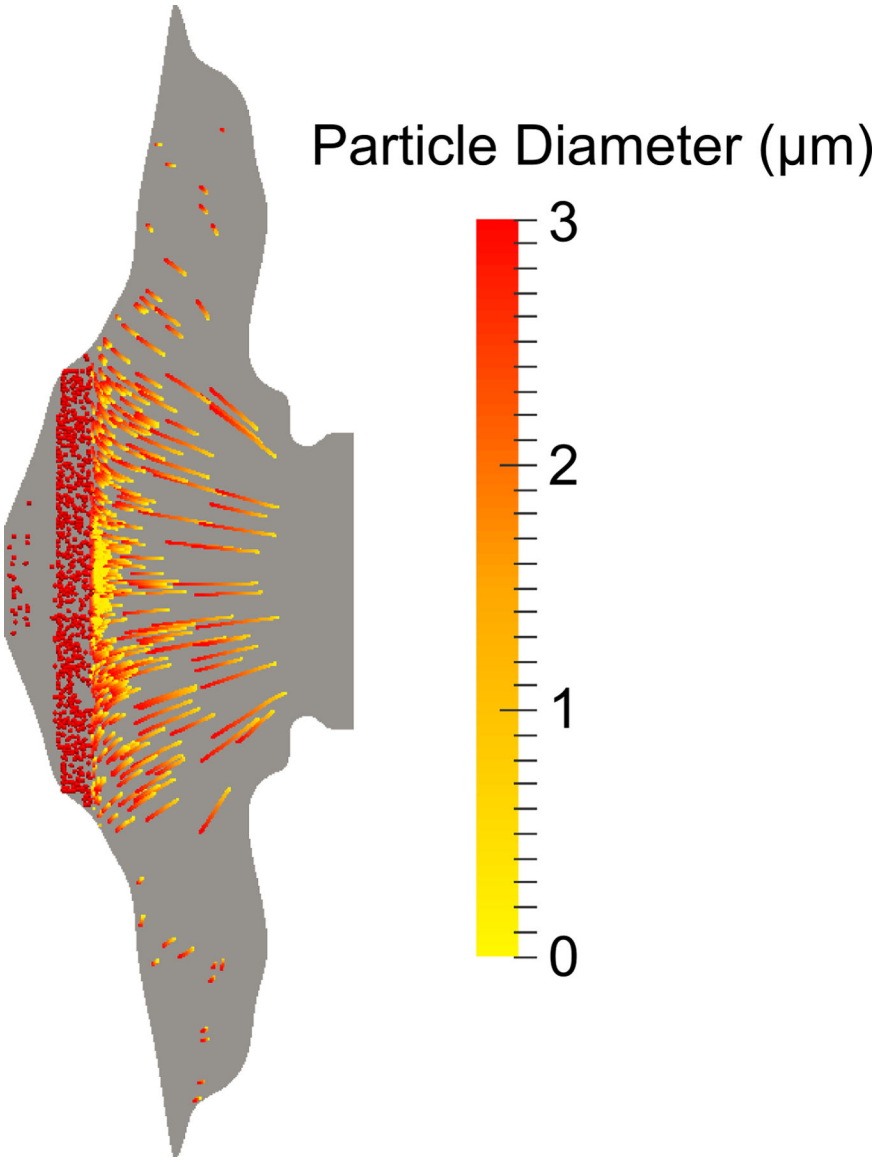

Figure 4.
Particle pathlines, which show individual particle trajectories over the simulation time, are colored by current diameter as dissolution occurs.

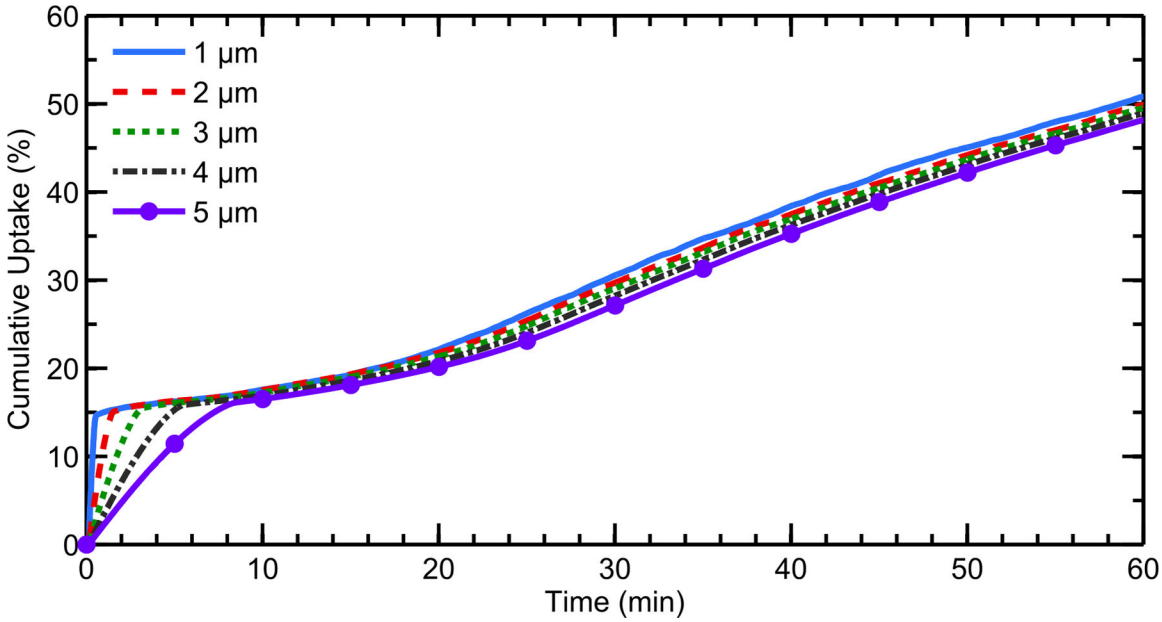

Figure 5.

Cumulative total nasal drug uptake at the epithelium over time is shown for varying initial particle diameters, a drug solubility Cs = 0.02 mg/mL, and a partition coefficient $K_{o/w}$ = 5000. Results are shown as a percentage of total injected drug mass.

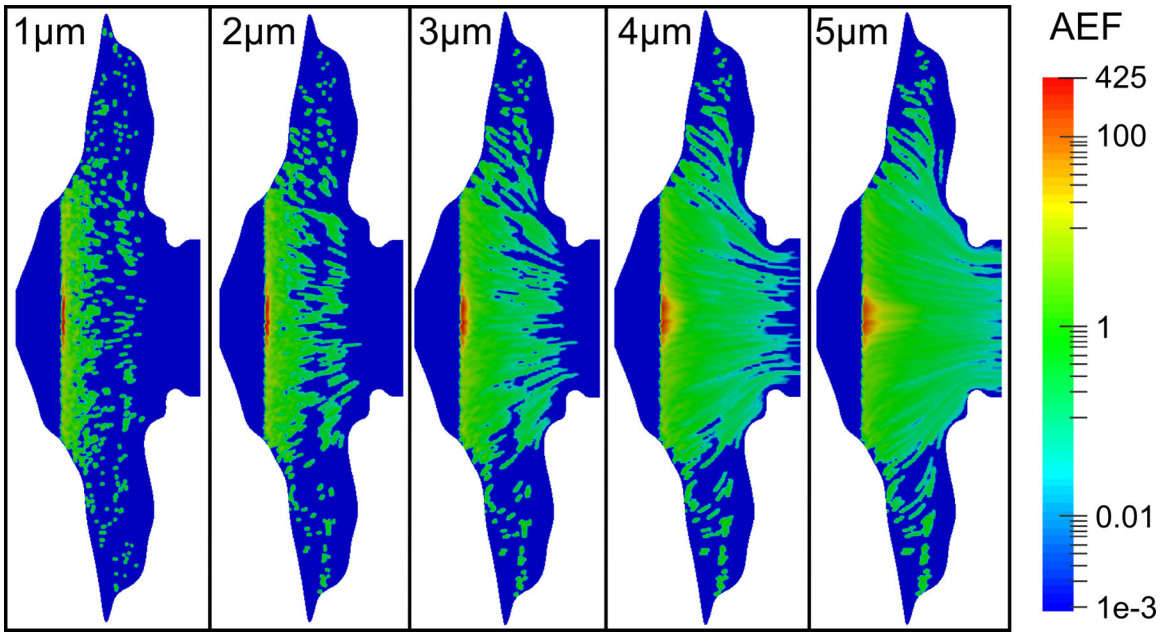

Figure 6.

Contours of the AEF are shown for varying initial particle diameters, a drug solubility of C_s = 0.02 mg/mL, and a partition coefficient $K_{o/w}$ = 5000.

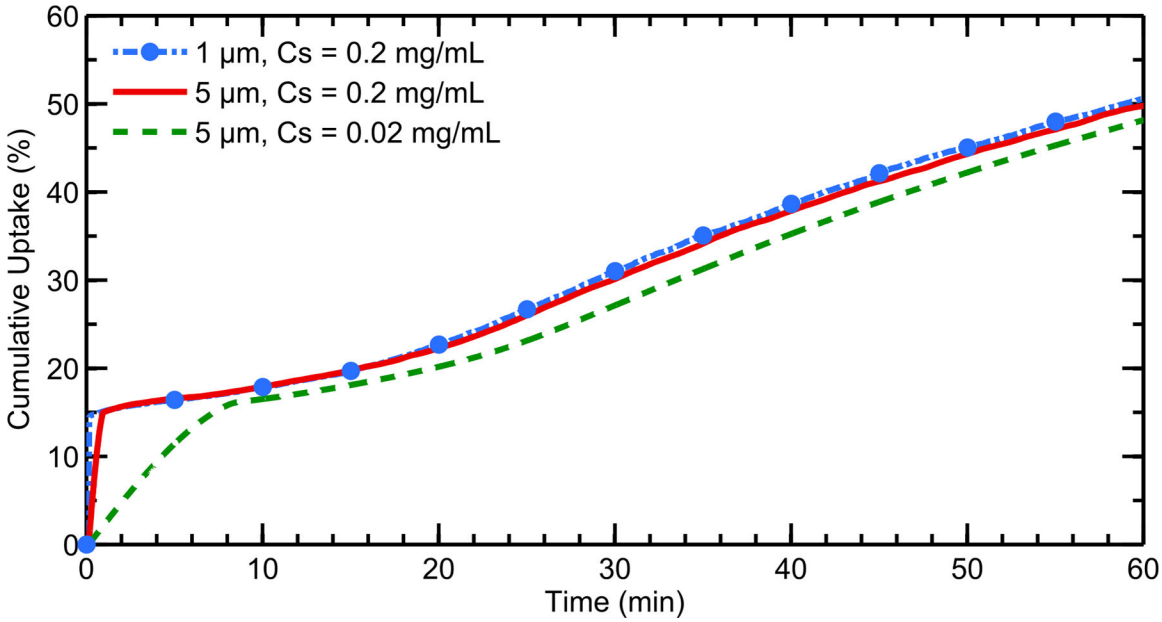

Figure 7.

Cumulative total nasal drug uptake at the epithelium over time is shown for varying drug solubilities and initial particle diameters with a constant partition coefficient of $K_{o/w} = 5000$. Results are shown as a percentage of total injected drug mass.

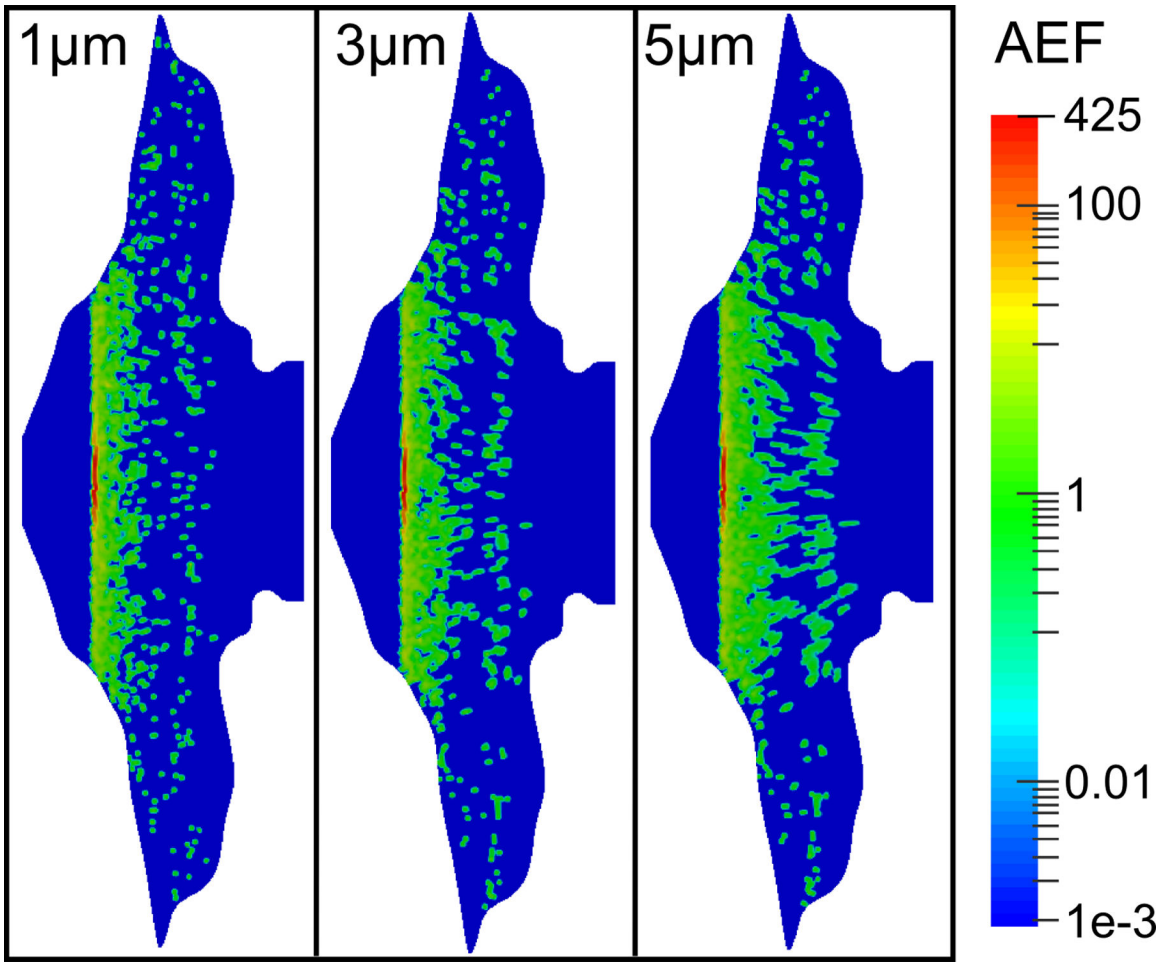

Figure 8.

Contours of the AEF are shown for varying initial particle diameters, a drug solubility Cs = 0.2 mg/mL, and a partition coefficient $K_{o/w}$ = 5000.

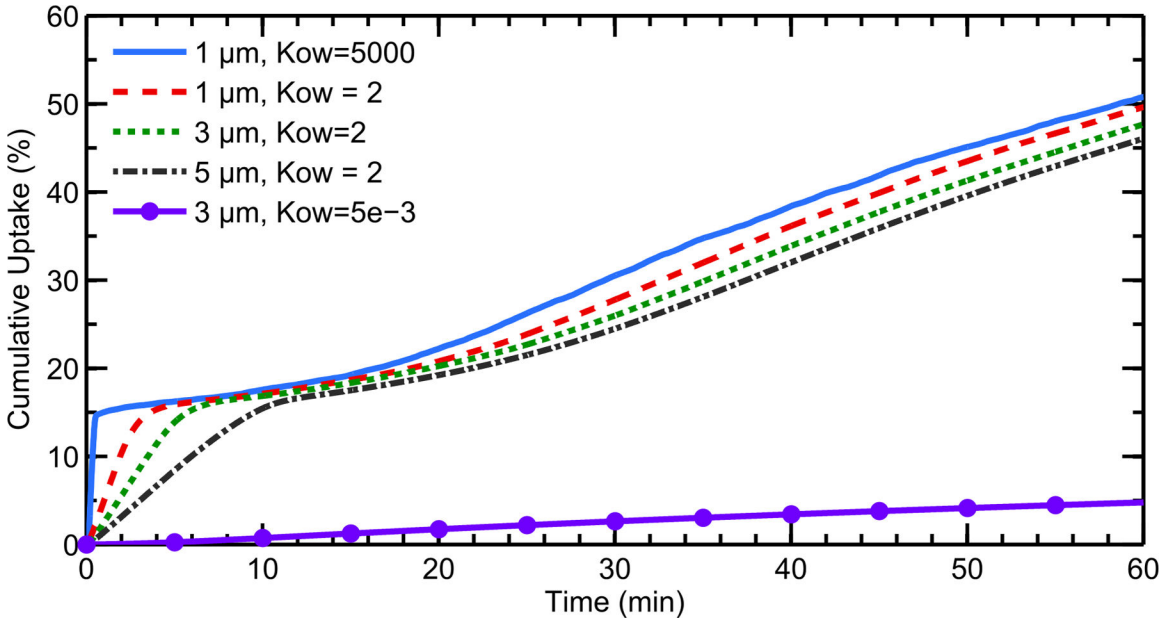

Figure 9.

Cumulative total nasal drug uptake at the epithelium over time is shown for varying drug partition coefficients ($K_{o/w}$) and initial particle diameters, with a constant solubility of C_s = 0.02 mg/mL. Results are shown as a percentage of total injected drug mass.

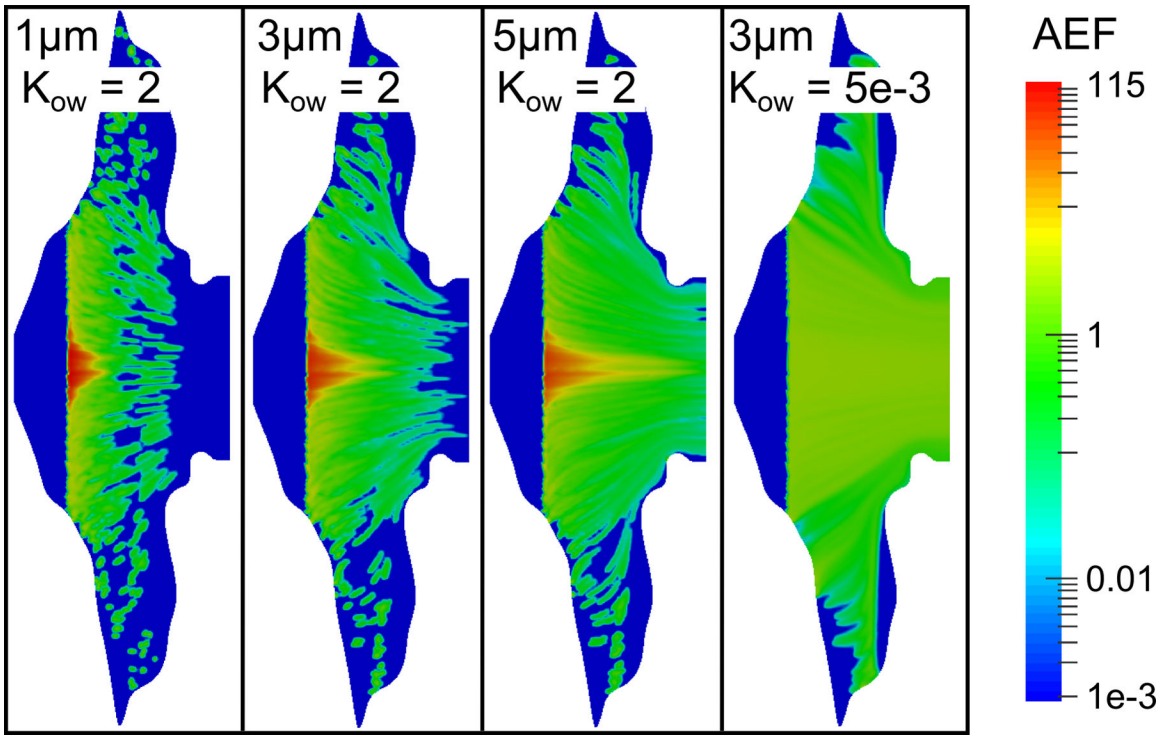

Figure 10.

Contours of the AEF are shown for varying initial particle diameters and drug partition coefficients (K_{ow}), with a constant drug solubility of Cs = 0.02 mg/mL.

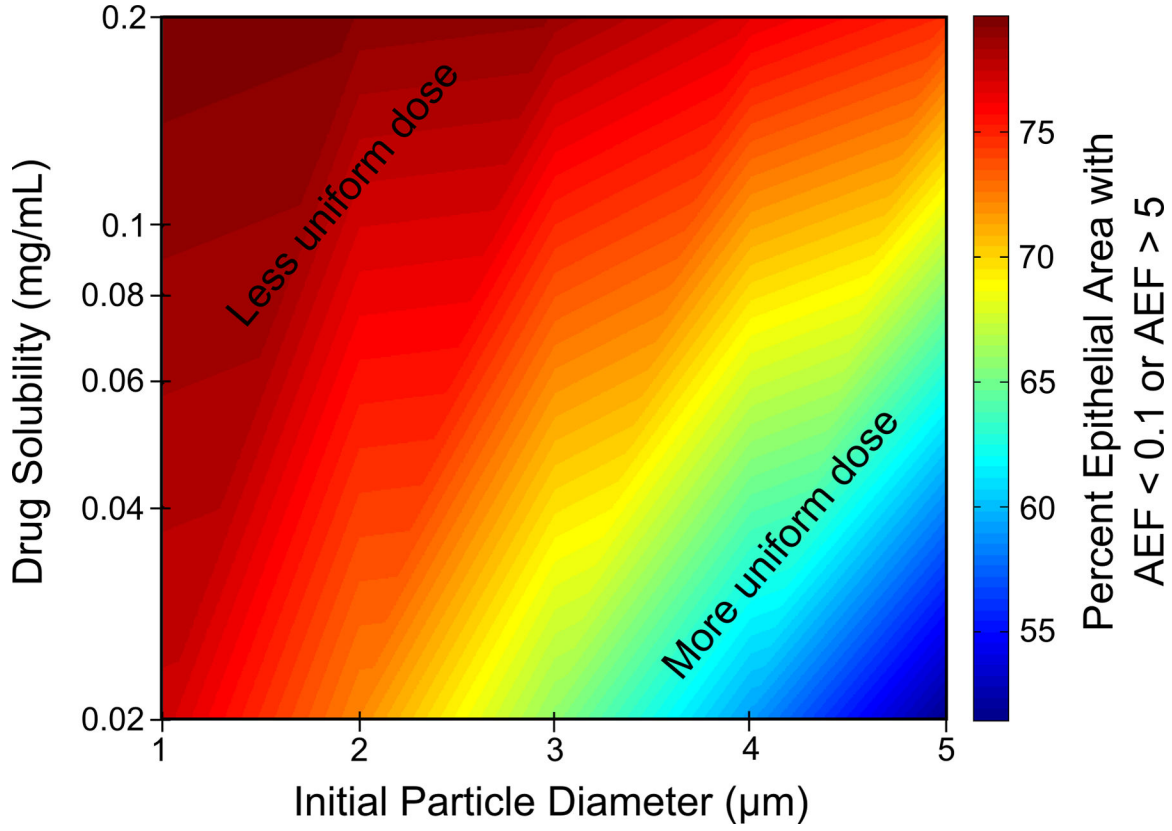

Figure 11.

Percent of the epithelial surface area with an AEF < 0.1 or AEF > 5 as a function of initial particle diameter and aqueous drug solubility for a partition coefficient of $K_{o/w} = 5000$.

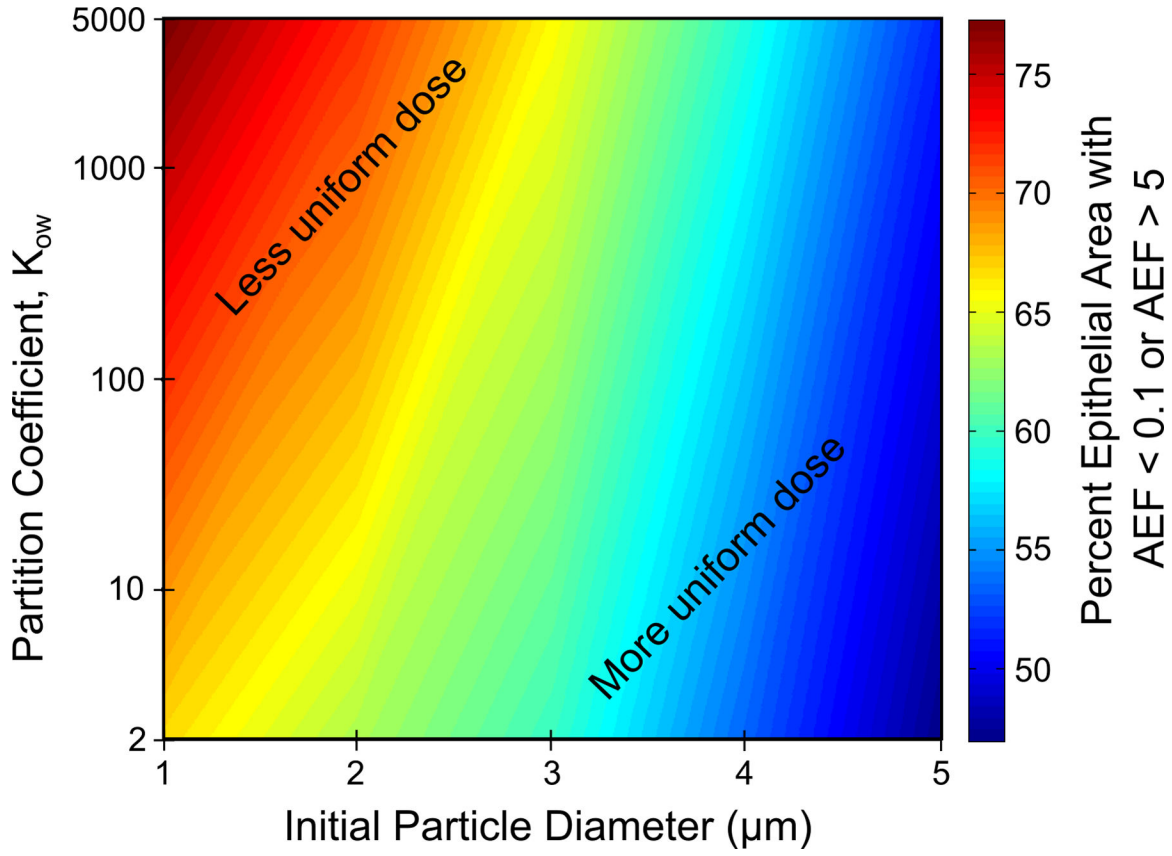

Figure 12.

Percent of the epithelial surface area with an AEF < 0.1 or AEF > 5 as a function of initial particle diameter and drug partition coefficient for a drug solubility of Cs = 0.02 mg/mL.